

# Mechanochemical Synthesis of Nanocrystalline Nickel–Molybdenum Compounds, Their Morphology and Application in Catalysis: I. Effect of the Ni : Mo Atomic Ratio on the Structure and Properties of Nickel–Molybdenum Compounds Prepared under Mechanochemical Synthesis Conditions

O. A. Knyazheva<sup>a</sup>, O. N. Baklanova<sup>a, b</sup>, A. V. Lavrenov<sup>a</sup>, V. A. Drozdov<sup>a, b</sup>, N. N. Leont'eva<sup>a</sup>,  
M. V. Trenikhin<sup>a</sup>, A. B. Arbuzov<sup>a</sup>, and V. A. Likhholobov<sup>a, b</sup>

<sup>a</sup> Institute of Hydrocarbon Processing, Siberian Branch, Russian Academy of Sciences, Omsk, 644040 Russia

<sup>b</sup> Omsk State Technical University, Omsk, Russia

e-mail: knyazheva@ihcp.oscsbras.ru

Received November 2, 2010

**Abstract**—Mechanochemical activation in high-energy planetary activators was used for the preparation of highly dispersed nickel–molybdenum compounds. Nickel hydroxocarbonate  $[\text{NiCO}_3 \cdot 2\text{Ni}(\text{OH})_2 \cdot n\text{H}_2\text{O}]$  and ammonium paramolybdate  $[(\text{NH}_4)_6\text{Mo}_7\text{O}_{24} \cdot 4\text{H}_2\text{O}]$  were chosen as starting compounds. The effect of the Ni : Mo atomic ratio on the composition and structure of products formed in the process of mechanochemical activation followed by calcination was studied. It was found that, at the Ni : Mo atomic ratios of 1.0 and 1.4, the mechanically activated product after calcination at 520°C contained 70–100%  $\beta$ - $\text{NiMoO}_4$ , which is a stable phase at temperatures lower than 180°C.

**DOI:** 10.1134/S0023158411060097

## INTRODUCTION

It is well known [1] that, depending on preparation procedures, the nickel–molybdenum systems with different Ni : Mo atomic ratios can be represented as the following compounds:

- (1) Ni(II) and Mo(VI) oxides ( $\text{NiO}$  and  $\text{MoO}_3$ );
- (2) stoichiometric nickel molybdate ( $\alpha$ - $\text{NiMoO}_4$ ), which is a low-temperature modification stable at room temperature, where molybdenum and nickel atoms are octahedrally coordinated [2–4];
- (3) stoichiometric nickel molybdate ( $\beta$ - $\text{NiMoO}_4$ ), which is a high-temperature modification stable at temperatures higher than 180°C, where molybdenum atoms occur in tetrahedral positions [2, 3];
- (4) nonstoichiometric nickel molybdate (a  $\beta$ - $\text{NiMoO}_4$ – $\text{NiO}$  solid solution), which is formed upon the interaction of the high-temperature modification with superstoichiometric nickel oxide and stable at room temperature [3].

As follows from published data, the catalytic properties of nickel molybdates are closely related to their structure [5]. Thus, for instance, it was shown that the selectivity of  $\beta$ - $\text{NiMoO}_4$  in the reaction of propane dehydrogenation to propene is higher (by a factor of more than 2) than that of the  $\alpha$  phase. In particular, Chaturvedi et al. [6] found that the  $\text{Mo}^{6+}$  ion in a tetrahedral environment in the  $\beta$  phase is coordinatively

unsaturated and its free  $4d$  orbitals are destabilized to a lesser degree than in an octahedral environment. This can contribute to the appearance of interactions between the  $4d$  orbitals of Mo and the occupied orbitals of hydrocarbons (in partial oxidation reactions) or mercaptans (hydrodesulfurization reactions). Because of this, the  $\beta$  phase is more chemically active than the  $\alpha$  phase. In a series of publications [7–10], which were devoted to a study of the catalytic properties of sulfidized  $\text{NiMoO}_4$  compounds, it was reported that sulfide catalysts based on  $\beta$ - $\text{NiMoO}_4$  exhibited the best catalytic properties in the reaction of dibenzothiophene hydrodesulfurization. It was found that the formation of Mo sulfides in the sulfidization of  $\beta$ - $\text{NiMoO}_4$  occurred more intensely than in the sulfidization of  $\alpha$ - $\text{NiMoO}_4$ . This difference in the ability to form sulfides makes  $\beta$ - $\text{NiMoO}_4$  a better precursor than  $\alpha$ - $\text{NiMoO}_4$  for the preparation of hydrofining catalysts.

Plyasova et al. [3] demonstrated that  $\beta$ - $\text{NiMoO}_4$  can also be formed at room temperature at a nonstoichiometric ratio between Ni and Mo, for example, at Ni : Mo = 1.2–2.0. In this case, they considered the formation of a solid solution of  $\text{NiO}$  in  $\text{NiMoO}_4$ , which makes the tetragonal modification of Mo stable at low temperatures.

In the last decade, highly dispersed bulk catalysts based on Ni and Mo for the use in slurry processes for

the conversion of heavy oils have been intensely developed [11].

Effective highly dispersed catalysts can be obtained with the use of nontraditional technological innovations. Mechanochemical activation applied to the synthesis of active catalyst structures can be a process of this kind. Molchanov and Buyanov [12] demonstrated in a review that the activity and selectivity of catalysts increased after mechanochemical activation. For example, it was established that the treatment of molybdenum disulfide in a vibrating mill changed its selectivity in the hydrodesulfurization reaction of thiophene etc. Huirache-Acuna et al. [13] synthesized a Ni–Mo–W catalyst for hydrodesulfurization upon the joint mechanically activated treatment of the above metals in a Spex 8000 high-energy mill in an inert atmosphere for 6–9 h. The resulting composite was sulfidized and tested in a model reaction of dibenzothiophene hydrodesulfurization; it exhibited satisfactory results comparable with those for commercial supported catalysts.

It is most reasonable to organize a mechanochemical activation process so that to combine the mechanical action on a reaction mixture with the acid–base interaction of individual components under hydrothermal conditions created upon the release of hydration water, that is, under mild mechanochemical synthesis conditions [14].

This work was devoted to a study of bulk highly dispersed catalyst precursors for hydrogenation processes based on metal (Ni and Mo) compounds synthesized with the use of mechanochemical activation followed by thermal treatment. The use of highly reactive hydrated salts such as ammonium paramolybdate and nickel hydroxocarbonate, which exhibit acidic and basic properties, respectively, for the synthesis of Ni–Mo catalyst precursors is an important distinguishing characteristic of this technology.

In this work, we studied the effects of the composition of a mechanically activated mixture and the mechanochemical activation process parameters on the composition and structure of Ni–Mo products after the stage of mechanochemical activation followed by thermal treatment.

As a result of this study, we obtained relationships between the chemical and phase composition, texture, and morphology of mechanically activated materials and changes in the composition of initial reaction mixtures. The results can be represented as individual stages, which will be considered in special publications.

(1) Effect of the Ni : Mo atomic ratio on the structure and properties of nickel–molybdenum compounds obtained by mechanochemical activation and thermal treatment.

(2) Effect of mechanochemical activation parameters (process power density and exposure time) on the

phase composition and structure of nickel–molybdenum compounds after mechanochemical activation.

(3) The electron-microscopic study of bulk Ni–Mo sulfide catalysts for hydrogenation processes synthesized by mechanochemical activation.

(4) Catalytic properties of bulk Ni–Mo sulfide catalysts for hydrogenation processes prepared with the use of mechanochemical activation in the model reactions of methylnaphthalene and dibenzothiophene decomposition.

## EXPERIMENTAL

In the course of the experimental studies, the following salts were chosen as starting compounds for the synthesis of nickel molybdate by mechanochemical activation: nickel hydroxocarbonate (NHC)  $\text{NiCO}_3 \cdot 2\text{Ni}(\text{OH})_2 \cdot n\text{H}_2\text{O}$  (Aldrich) and ammonium paramolybdate (APM)  $(\text{NH}_4)_6\text{Mo}_7\text{O}_{24} \cdot 4\text{H}_2\text{O}$  (Sigma-Aldrich).

The mechanochemical activation of NHC and APM mixtures with different Ni : Mo atomic ratios ( $m$ ) of 0.3, 1.0, 1.4, and 3.3 was performed in an AGO-2S water-cooled planetary mill with a centripetal acceleration of 300 m/s<sup>2</sup>. Steel balls 8 mm in diameter were used as grinding bodies. The weight of balls loaded into drums was 170 g; the weight of an activated sample was 2.5 g, and the weight ratio between the raw material and grinding bodies was 1 : 70. The mechanochemical activation time of 15 min was chosen based on the results obtained previously [15].

The concentrations of Ni and Mo in the mechanically activated samples were determined by atomic absorption spectrometry (AAS) on an AA-6300 instrument (Shimadzu).

To study physicochemical transformations in the course of mechanochemical activation, the samples with different Ni : Mo atomic ratios were examined by synchronous thermal analysis with mass spectrometry (STA–MS), X-ray diffraction (XRD) analysis, transmission electron microscopy (TEM), and IR spectroscopy.

The starting reagents and samples after mechanochemical activation were analyzed by STA–MS on an STA-449C instrument (Netzsch) coupled with a quadrupole mass spectrometer. The test temperature range was 40–900°C; the heating was performed in a flow (70 ml/min) of a gas containing 20% O<sub>2</sub> in Ar (gas purity of 99.999%). Ions with  $m/z$  17 (NH<sub>3</sub><sup>+</sup>), 18 (H<sub>2</sub>O<sup>+</sup>), and 44 (CO<sub>2</sub><sup>+</sup>) were detected by mass spectrometry. The results were processed using the Proteus program.

XRD analysis was performed on a D8 Advance diffractometer (Bruker). The concentrations of individual phases were semiquantitatively evaluated based on diffraction data from the PDF file with the use of the EVA program package. This analysis implies that all of

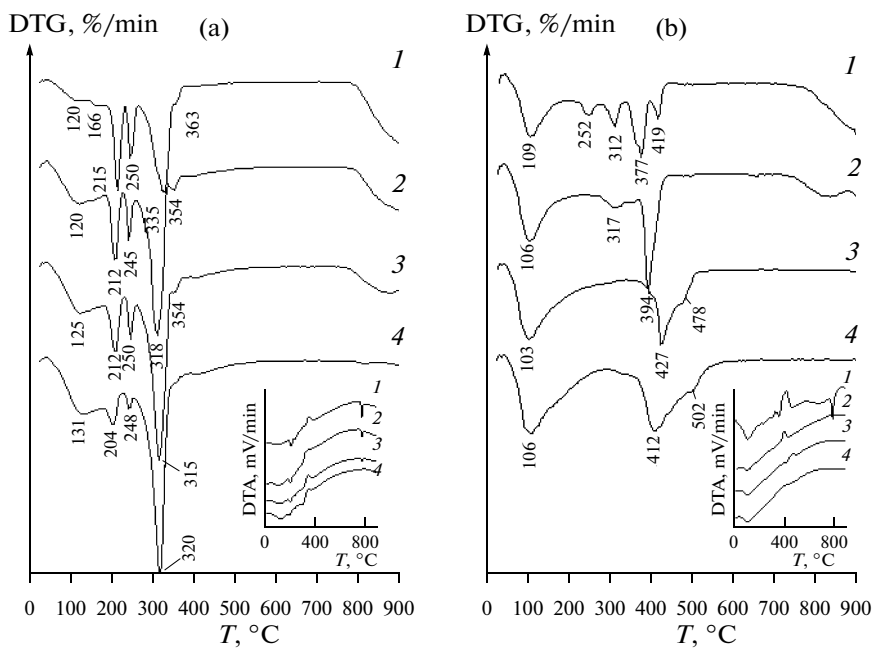


**Fig. 1.** DTG curves for the (a) initial and (b) mechanically activated mixtures of NHC and APM at the following Ni : Mo atomic ratios  $m$ : (1) 0.3, (2) 1.0, (3) 1.4, and (4) 3.3. Insets: DTA curves for corresponding samples.

the phases are well crystallized and identified and their sum is 100%. Additionally, high-temperature X-ray studies were performed on the D8 Advance instrument in an HTK-16 high-temperature chamber (Anton Paar). The heating rate was 5°C/min. The delay time before measuring each particular diffraction pattern was 15 min.

The electron-microscopic studies were performed on a JEM-2100 transmission electron microscope (JEOL) with an accelerating voltage of 200 kV and a crystal lattice resolution of 0.14 nm, which was equipped with an INCA 250 energy-dispersive X-ray spectrometer (Oxford Instruments).

The IR spectra of the initial and mechanically activated calcined samples were measured on a Nicolet 5700 instrument (Thermo Fisher Scientific). The samples were mixed with KBr powder and pressed as pellets, and the IR spectra were measured with a resolution of 4  $\text{cm}^{-1}$  and a spectrum accumulation number of 32.

The specific surface area was determined by an adsorption method on a Sorptomatic 1900 instrument (Carlo Erba).

## RESULTS AND DISCUSSION

At the first stage of this work, we determined the concentrations of metals in mechanically activated samples with different Ni : Mo atomic ratios by AAS and calculated ratios between them. The experimental results showed that the concentrations of metals in the mixtures and the Ni : Mo ratios after mechanochemical activation coincided with the calculated values.

We used STA-MS to evaluate the occurrence of solid-phase reactions between NHC and APM. The curves of differential thermogravimetric analysis (DTG) for the individual compounds NHC and APM were published previously [15]. Figure 1 shows the DTG curves for the mixtures of NHC and APM at Ni : Mo atomic ratios of 0.3, 1.0, 1.4, and 3.3 (a) before and (b) after mechanochemical activation.

As can be seen in Fig. 1a, the mixtures of NHC and APM exhibited weight loss peaks characteristic of individual NHC and APM in the temperature range of 40–370°C [15]. The positions of these peaks and the ratio between their intensities changed insignificantly upon changes in the composition of the mixture. At temperatures higher than 770–790°C, the DTG curves for the initial mixtures of NHC and APM (Fig. 1a) exhibited a weight loss due to the sublimation of  $\text{MoO}_3$ .

The shapes of the DTG curves (Fig. 1b) obtained for the mechanically activated mixtures of NHC and APM with different Ni : Mo atomic ratios differed from those for the initial mixtures. Firstly, the DTG curve exhibited a weight loss peak due to crystal water in the temperature range of 103–109°C, which is substantially lower in terms of temperature than that for the initial mixtures (120–130°C). Most likely, the shift of this peak for the mechanically activated mixtures toward lower temperatures resulted from the disintegration of primary particles, that is, an increase in the external surface, and the degradation of crystal hydrate complexes with the transfer of water to an adsorbed state.

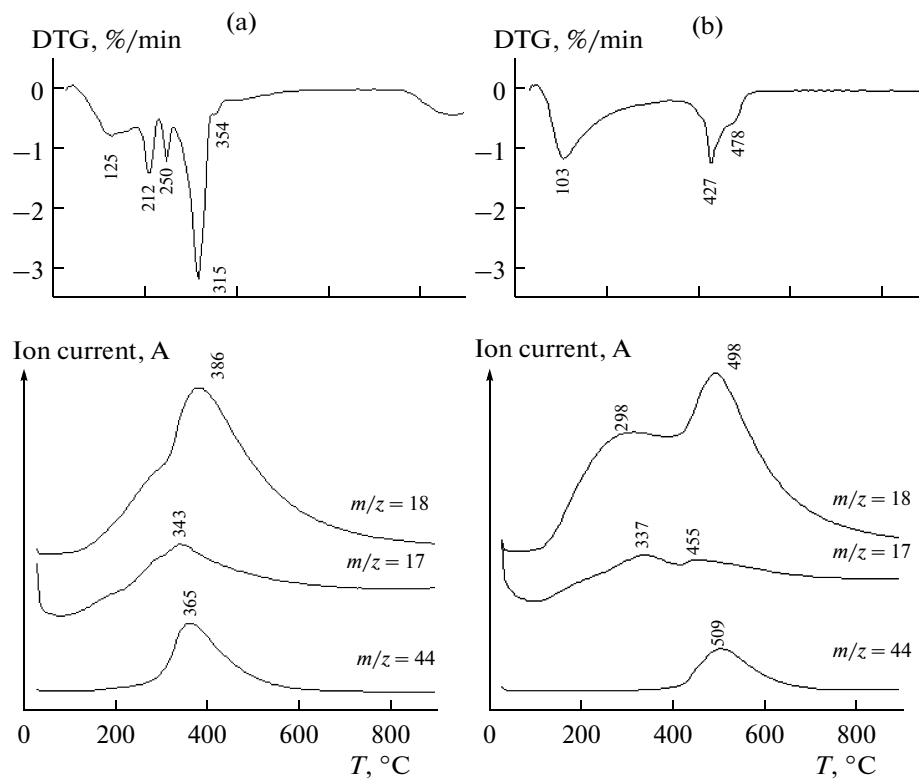


**Fig. 2.** Mass spectra of the decomposition of a mixture of NHC and APM with the atomic ratio  $\text{Ni} : \text{Mo} = 1.4$  in air (a) before and (b) after mechanochemical activation, where  $m/z = 17$  ( $\text{NH}_3^+$ ),  $m/z = 18$  ( $\text{H}_2\text{O}^+$ ), and  $m/z = 44$  ( $\text{CO}_2^+$ ).

Secondly, DTG peaks characteristic of the individual compounds were not detected in the temperature range of 100–380°C. Only at the atomic ratio  $\text{Ni} : \text{Mo} = 0.3$ , the characteristic DTG peaks of APM decomposition were observed in this region. It is obvious that, in this sample, an excess portion of APM did not react with NHC.

Thirdly, the DTG curves for the mechanically activated mixtures exhibited an additional weight loss peak in the temperature range of 410–425°C; this peak was absent from the DTG curves for the initial mixtures of the corresponding composition. Usually, a peak in this temperature range is related to the decomposition of a complex double salt accompanied by the removal of ammonia and water [3, 16].

The differential thermal analysis (DTA) curves of mechanically activated samples exhibited exo effects in the temperature range of 400–430°C; according to published data, these effects can be due to the crystallization of nickel molybdates. Plyasova et al. [3] reported that an increase in the nickel content leads to a shift in the exo effect toward higher temperatures. In this case, according to Madeira et al. [16], the degree of crystallinity decreases. It is believed that this is due to the formation of a solid solution of  $\text{NiO}$  in  $\text{NiMoO}_4$ . Note that, unlike samples with other atomic ratios between the metals, the mechanically activated sam-

ple with  $m = 0.3$  exhibited an endo effect related to the melting of  $\text{MoO}_3$  in the region of 790°C in the DTA curve (Fig. 1b, insert). A further increase in the temperature leads to the sublimation of  $\text{MoO}_3$ , as evidenced by a weight loss in the DTG curve (Fig. 1b).

Figure 2 shows the DTG curves and mass spectra of a mixture of NHC and APM with  $m = 1.4$  before and after mechanochemical activation. The composition of the released gas-phase products corresponds to  $\text{NH}_3$ ,  $\text{H}_2\text{O}$ , and  $\text{CO}_2$ , detected by the ion currents of  $\text{NH}_3^+$ ,  $\text{H}_2\text{O}^+$ , and  $\text{CO}_2^+$ , respectively. The given spectra illustrate the fact that a shift of maximum signals toward higher temperatures of 60–455°C is characteristic of the mechanically activated sample, as compared with the initial mixture (40–390°C).

As can be seen in Fig. 2a, according to mass-spectrometric data, water is released from the initial mixture of NHC and APM in the region of 110–900°C, and the curve exhibits a maximum at 386°C and a shoulder in the low-temperature region (110–300°C). The release of water is due to the decomposition and dehydration of NHC and APM. In the mechanically activated mixture (Fig. 2b), the release of water occurs in the temperature range of 110–900°C. In this case, the curve exhibits two peaks: the first peak at 298°C and the second at 498°C. The peak asymmetry and the increase in the temperature at which a maximum of

**Table 1.** Thermal analysis data for the initial and mechanically activated mixtures of NHC + APM at different Ni : Mo atomic ratios

Ni : Mo atomic ratio ( <i>m</i> )	Weight loss in the temperature range, %					
	initial mixture			after mechanochemical activation		
	40–520°C	520–900°C	40–900°C	40–520°C	520–900°C	40–900°C
0.3	20.2	6.9	27.1	18.6	6.2	24.8
1.0	24.3	4.8	29.1	20.5	4.2	24.7
1.4	29.3	3.9	33.2	20.7	0.5	21.2
3.3	30.0	0.6	30.6	25.4	0.7	26.1

water release was observed to 498°C suggest the occurrence of water in two forms: adsorbed water is a portion of water, and the other portion is structurally bound water; that is, it occurs in the structure of the compound and larger energy should be delivered to remove this water.

Ammonia is released as a thermal decomposition product from the initial and mechanically activated samples. For the initial sample (Fig. 2a), the shape of the mass spectrum of the release of  $\text{NH}_3^+$  ( $m/z = 17$ ) is almost symmetrical, and a maximum is observed at a temperature of 343°C. The curve of the mechanically activated sample (Fig. 2b) for ammonia exhibits two peaks, and the temperature of the second maximum is 455°C. It is believed that a portion of released ammonia corresponds to the structurally bound  $\text{NH}_4^+$  ion.

The decomposition of NHC with the release of water and  $\text{CO}_2$  [15] occurs in the temperature range of 50–370°C; in this case, two endo effects are observed. The mass spectrum of the initial mixed sample with  $m/z = 44$  ( $\text{CO}_2^+$ ) (Fig. 2a), which corresponds to the release of  $\text{CO}_2$ , has a symmetrical shape with a maximum at 365°C. The mass spectrum of the mechanically activated sample with  $m/z = 44$  ( $\text{CO}_2^+$ ) exhibits a peak at a temperature of 509°C; in this case, the shape of the spectrum is analogous to the shape of the mass spectrum of  $\text{CO}_2$  for the unactivated initial sample.

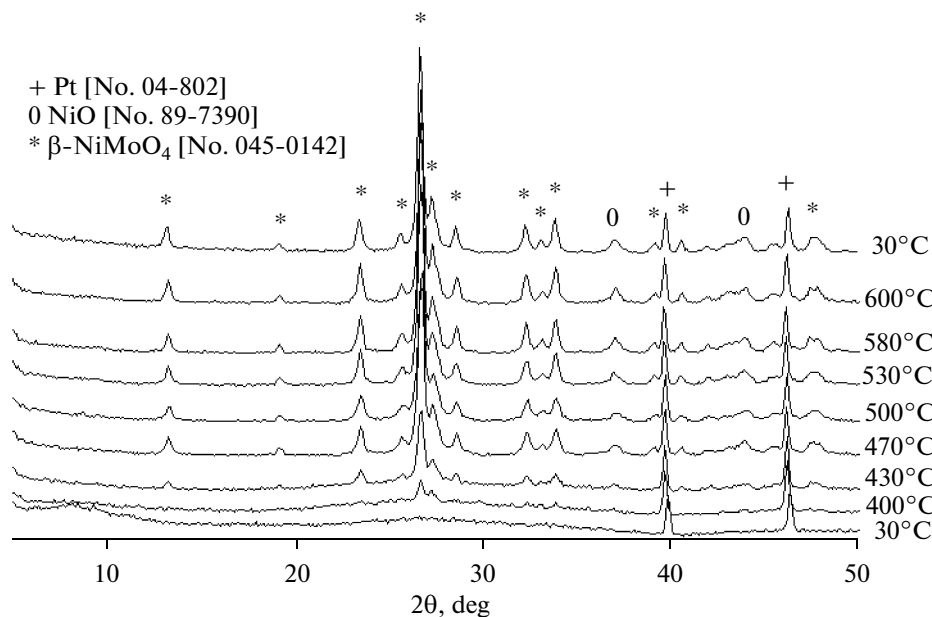
Note that the shapes of the mass spectra remain unchanged at other Ni : Mo atomic ratios in the test samples.

Table 1 summarizes the results obtained by STA-MS and shown in Figs. 1 and 2: the weight losses detected in the temperature ranges of 40–520, 520–900, and 40–900°C for the initial and mechanically activated mixtures of NHC and APM at different values of *m* are given. The temperature ranges were chosen based on the fact that the weight loss at temperatures to 520°C is related to the decomposition and depolymerization reactions of NHC and APM and the removal of components such as  $\text{CO}_2$ ,  $\text{NH}_3$ , and  $\text{H}_2\text{O}$ . The weight loss at temperatures higher than 520°C is

mainly related to the sublimation of  $\text{MoO}_3$ . Table 1 indicates that an increase in the Ni : Mo atomic ratio from 0.3 to 3.3 in the composition leads to a monotonic increase in the weight loss in the temperature range of 40–520°C and a decrease in the weight loss at temperatures of 520–900°C for the initial and mechanically activated compositions. This can be related to a change in the composition of volatile products (an increase in the fraction of  $\text{CO}_2$ ) and a decrease in the amount of free molybdenum oxide in the mixture. Similar regularities are also retained for the compositions after mechanochemical activation.

A comparison between weight losses for the initial mixtures and the mechanically activated compositions shows that the weight losses decreased after mechanochemical activation for all of the values of *m* by 1.6–8.6% in the temperature range of 40–520°C or by 0.7–3.4% in the temperature range of 520–900°C. The observed decrease in weight losses for the mechanically activated compositions suggests the occurrence of solid-phase reactions between NHC and APM in the course of mechanochemical activation. Special attention should be focused on the composition with *m* = 1.4. It exhibited the greatest change in weight losses in the course of mechanochemical activation: the weight loss decreased after mechanochemical activation by 8.6% in the range of 40–520°C or by 3.4% in the range of 520–900°C. The experimental results allow us to assume that solid-phase reactions occur most completely in the course of the mechanochemical activation of a mixture of NHC and APM at the atomic ratio Ni : Mo = 1.4.

Figure 3 shows the results of the in situ high-temperature X-ray studies of the mechanically activated mixture with Ni : Mo = 1.4 on heating in the range of 30–600°C and cooling in the range of 600–30°C. As can be seen in thermal diffraction patterns, the formation of the complex salt  $\beta\text{-NiMoO}_4$  and the oxide phase  $\text{NiO}$  was detected at a temperature higher than 470°C. An increase in the temperature to 600°C leads to an increase in the degree of crystallinity of the above compounds. Upon the subsequent cooling down to 30°C, both of the phases remain in the sample. Previously, Mazzocchia et al. [4] described similar thermal stability of  $\beta\text{-NiMoO}_4$  for nonstoichiometric mixtures



**Fig. 3.** Results of the evaluation of the phase composition of a mixture of NHC and APM with the atomic ratio Ni : Mo = 1.4 after mechanochemical activation according to XRD patterns obtained in a high-temperature chamber (the temperatures are specified in the figure).

at the ratios Ni : Mo > 1. Mazzocchia et al. [4] explained the observed thermal stability of  $\beta$ -NiMoO<sub>4</sub> at low temperatures by the formation of an interstitial solid solution of nickel oxide in the lattice of NiMoO<sub>4</sub>.

Figure 4 shows the diffraction patterns of the (a) initial and (b) mechanically activated mixtures of NHC and APM with different values of  $m$ . All of the samples were calcined at 520°C in air before analysis. As can be seen, the diffraction patterns of the initial mixtures of NHC and APM exhibit the presence of only the crystalline oxides NiO and MoO<sub>3</sub> at all values of  $m$ . Only the intensities of individual peaks change with  $m$ . The shape of the diffraction patterns of the mechanically activated samples considerably changes with changing the composition of the mixture. The diffraction pattern of the mechanically activated mixture with  $m = 0.3$  exhibits peaks due to crystalline MoO<sub>3</sub> and no peaks due to crystalline nickel oxide. In this case, the presence of  $\alpha$ - and  $\beta$ -NiMoO<sub>4</sub> is noted.

The diffraction pattern of the sample with  $m = 1.0$  also exhibits reflections due to the phases of  $\alpha$ -NiMoO<sub>4</sub> and  $\beta$ -NiMoO<sub>4</sub> with the predominance of the latter. In this case, the formed phase of  $\alpha$ -NiMoO<sub>4</sub> is stoichiometric nickel molybdate, whereas the phase of  $\beta$ -NiMoO<sub>4</sub> present in the sample has a nonstoichiometric composition. As the Ni content of the samples is increased, the amount of the  $\beta$ -NiMoO<sub>4</sub> phase increases and the crystallinity of the samples decreases. The latter manifests itself in the appearance of a halo in the 2θ region of 20–40° in the diffraction pattern of the sample and in an increase in the background level at  $m = 3.3$ . Obviously, this is related to the presence of an X-ray amorphous phase of nickel oxide

[16]. As can be seen in Fig. 4, the diffraction pattern of the sample with  $m = 3.3$  does not exhibit diffraction peaks over the entire range of scanned 2θ angles.

Table 2 summarizes the specific surface areas of the initial and mechanically activated NHC and APM and also mechanically activated mixtures of NHC and APM at the Ni : Mo atomic ratios of 1.0 and 1.4. As can be seen, NHC is characterized by a developed texture: the specific surface area of the initial NHC is 115 m<sup>2</sup>/g. Mechanochemical activation results in the disintegration of particles and the partial degradation of the porous texture: the specific surface area of the mechanically activated NHC decreases to 87 m<sup>2</sup>/g. APM can be ascribed to low-porous materials: the specific surface area of the initial APM is 6 m<sup>2</sup>/g, and it remains almost unchanged in the course of mecha-

**Table 2.** Specific surface areas  $S_{\text{BET}}$  of the initial compounds NHC and APM and their mechanically activated mixtures at Ni : Mo atomic ratios of 1.0 and 1.4 after calcination at 520°C

Sample	$S_{\text{BET}}$ , m <sup>2</sup> /g
NHC (initial)	115
NHC (mechanochemically activated)	87
APM (initial)	6
APM (mechanochemically activated)	6
NHC + APM (mechanochemically activated), Ni : Mo = 1.0	52
APM (mechanochemically activated), Ni : Mo = 1.4	19

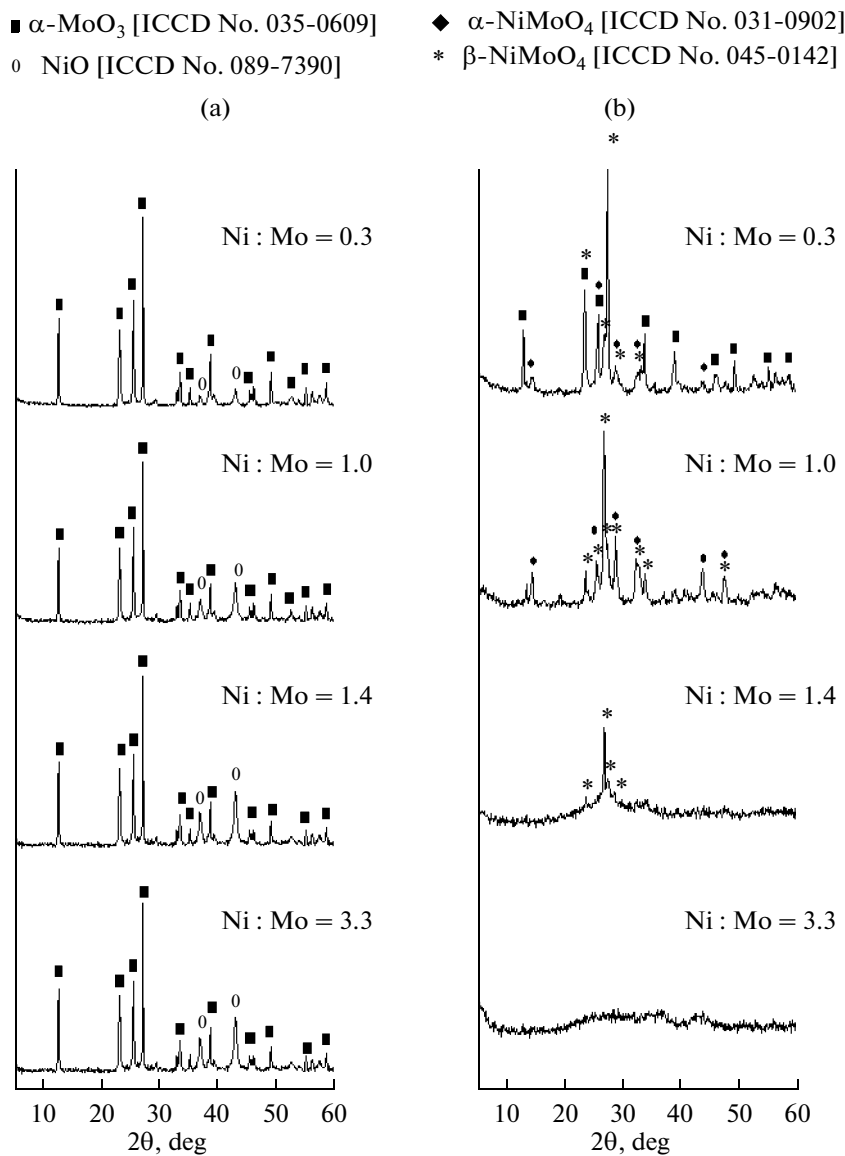


**Fig. 4.** Diffraction patterns of the (a) initial and (b) mechanically activated mixtures of NHC and APM with different Ni : Mo atomic ratios (all of the samples were calcined at 520°C before XRD analysis).

nochemical activation. The joint mechanical activation of NHC and APM leads to the production of composites with  $S_{\text{BET}}$  of 52 and 19  $\text{m}^2/\text{g}$ , respectively. Moreover, as follows from Table 2, the phase composition has a considerable effect on the specific surface area.  $S_{\text{BET}} = 52 \text{ m}^2/\text{g}$  for the sample that consists of a mixture of 18%  $\alpha\text{-NiMoO}_4$  and 82% of  $\beta\text{-NiMoO}_4$ . For the mechanically activated composite containing only the phase of  $\beta\text{-NiMoO}_4$ ,  $S_{\text{BET}}$  decreases to 19  $\text{m}^2/\text{g}$ .

Figure 5 shows the electron micrographs of the mechanically activated mixtures of NHC and APM with  $m = 1.4$  (a) before and (b) after calcination at 520°C. As can be seen in Fig. 5a, the mechanochemical activation of a mixture of NHC + APM results in the formation of characteristic agglomerates of pri-

mary particles, which are rounded plates, packed in uniform piles from 2 to 5 nm in sizes with a well-ordered structure.

The sample calcined at 520°C (Fig. 5b) is characterized by longer particles with individual faceted crystal details; in this case, the particle size increases to 20 nm or more, and the elemental composition of the synthesized sample is close to the calculated composition. The electron diffraction patterns and the diffraction patterns obtained by the Fourier transform are of point nature, which also suggests the high degree of coherence of their crystal lattices (Fig. 5b). According to TEM data, the crystal lattice planes with the indices (220) and (222) have periods of 0.336 and 0.264 nm, respectively, which are consistent with the theoretical values of 0.335 and 0.265 nm, respectively, character-

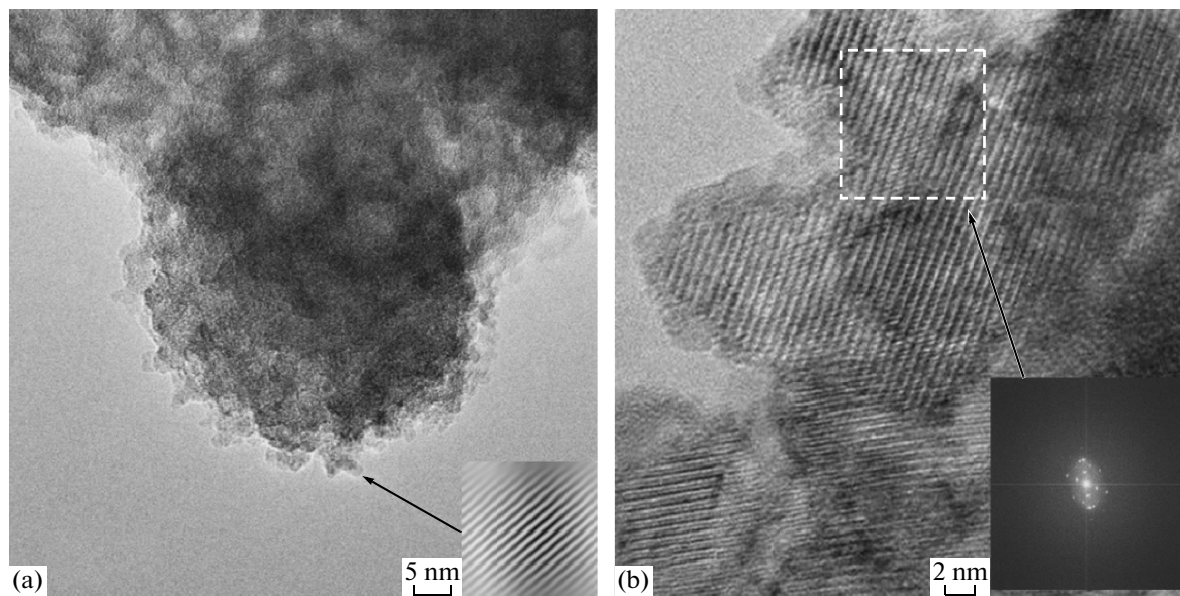


**Fig. 5.** Electron micrographs of the mechanically activated mixtures of NHC and APM with the atomic ratio  $\text{Ni} : \text{Mo} = 1.4$  (a) before and (b) after calcination at  $520^\circ\text{C}$ .

istic of  $\beta\text{-NiMoO}_4$  (ICCD, no. 45-0142). The TEM study confirmed the presence of the phase of  $\beta\text{-NiMoO}_4$  with a high degree of crystallinity.

Figure 6 shows the IR spectra of the mechanically activated and calcined samples with different values of  $m$ . In the IR spectrum of the sample with  $m = 0.3$  in the region of  $400\text{--}1150\text{ cm}^{-1}$ , absorption bands at 999, 956, and  $934\text{ cm}^{-1}$  are due to the stretching vibrations of terminal  $\text{Mo}=\text{O}$  bonds [16–18]; absorption bands at 853, 707, and  $594\text{ cm}^{-1}$  are due to the stretching vibrations of bridging  $\text{Mo}=\text{O}-\text{M}$  bonds (where  $\text{M}$  is  $\text{Ni}$  or  $\text{Mo}$ ) [1, 2], and an absorption band at  $443\text{ cm}^{-1}$  corresponds to the stretching vibrations of  $\text{Mo}=\text{O}$  and  $\text{Ni}=\text{O}$  bonds [16–18]. A comparison of the experimental IR spectrum with the published IR spectrum of crystalline  $\text{MoO}_3$  [19] shows a good agreement, and the presence of absorption bands at 956 and  $934\text{ cm}^{-1}$  suggests the occurrence of the phase of  $\alpha\text{-NiMoO}_4$ . As the nickel content of the mixture was increased to  $m = 1.0$ , absorption bands at 956 and  $934\text{ cm}^{-1}$  ( $\text{Mo}=\text{O}$ ); 883, 808, 707, and  $630\text{ cm}^{-1}$  ( $\text{Mo}=\text{O}-\text{Mo}$  and  $\text{Mo}=\text{O}-\text{Ni}$ ); and 443 and  $412\text{ cm}^{-1}$  ( $\text{Mo}=\text{O}$  and  $\text{Ni}=\text{O}$ ) appeared in the IR spectrum. The presence of characteristic absorption bands at 956, 934, and  $630\text{ cm}^{-1}$  indicates the formation of  $\alpha\text{-NiMoO}_4$ , and the presence of low-intensity absorption bands at 808 and  $883\text{ cm}^{-1}$  suggests the presence of small amounts of  $\beta\text{-NiMoO}_4$ . The experimental results support the XRD data. A further increase in the nickel content to the values of  $m = 1.4$  and 3.3 leads to the appearance of a group of wide insufficiently resolved absorption bands at 944 ( $\text{Mo}=\text{O}$ ); 880, 828, 798, and  $757\text{ cm}^{-1}$  ( $\text{Mo}=\text{O}-\text{Mo}$  and  $\text{Mo}=\text{O}-\text{Ni}$ ); and 431 ( $\text{Mo}=\text{O}$  and  $\text{Ni}=\text{O}$ ). It is likely that, according to Andrushkevich

et al. [20], these absorption bands correspond to the groups containing the  $\text{Mo}^{6+}$  ion in a tetrahedral coordination.

Thus, comparing the results of the comprehensive study of a mixture of NHC and APM by STA-MS, XRD analysis, IR spectroscopy, and TEM, we can conclude that the solid-phase reactions of the dehydration and destruction of the initial compounds occur in the course of the mechanochemical activa-

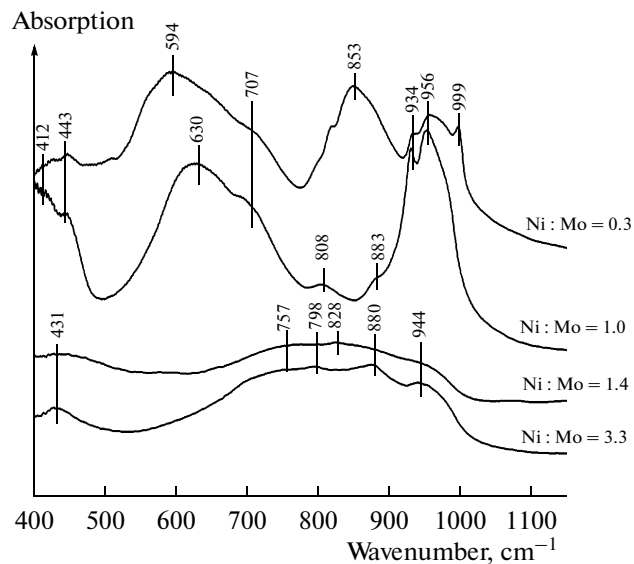


**Fig. 6.** IR spectra of the samples of the mixtures of NHC and APM with different  $\text{Ni} : \text{Mo}$  atomic ratios after mechanochemical activation followed by calcination at  $520^\circ\text{C}$ .

**Table 3.** Compositions of Ni LTM compounds prepared by mechanochemical activation and products obtained after their calcination at 520°C

Degree of nonstoichiometry $x$	Ni : Mo atomic ratio	Formula of the Ni LTM compound	Phase composition of the product after calcination at 520°C (based on XRD analysis and IR-spectroscopic data)	
			phase	amount, wt %
0	3.3	$(\text{NH}_4)\text{Ni}_3\text{O}(\text{OH})(\text{MoO}_4)_2 \cdot y_1\text{NiCO}_3$	NiO, $\beta\text{-NiMoO}_4$	— —
0.2	1.4	$(\text{NH}_4)\text{Ni}_{2.8}(\text{OH})_2(\text{MoO}_4)_2 \cdot y_2\text{NiCO}_3$	$\beta\text{-NiMoO}_4$	100
1.0	1.0	$(\text{NH}_4)\text{H}\text{Ni}_2(\text{OH})_2(\text{MoO}_4)_2 \cdot y_3\text{NiCO}_3$	$\alpha\text{-NiMoO}_4$ , $\beta\text{-NiMoO}_4$	18 82
2.4	0.3	$(\text{NH}_4)\text{H}_2\text{Ni}_{0.6}\text{O}(\text{OH})(\text{MoO}_4)_2 \cdot y_4\text{NiCO}_3$	MoO <sub>3</sub> , $\alpha\text{-NiMoO}_4$ , $\beta\text{-NiMoO}_4$	54 13 33

tion of the mixtures of NHC and APM at the values of  $m = 1.0$  and  $1.1$ . In this case, water, ammonia, and carbon dioxide are released with the formation of X-ray amorphous complex compounds. The calcination of these compounds at  $430\text{--}470^\circ\text{C}$  in air leads to their decomposition and the formation of nickel molybdates of different modifications ( $\alpha$  and  $\beta$ ). The chemical composition of these compounds was hypothesized. In this case, we considered that the nonstoichiometric precursors of transition metal molybdates [21] (so called layered transition metal molybdates or LTM compounds) have the general formula



where A is a transition metal (Ni in our case), and  $0 \leq x \leq 3/2$  is the degree of nonstoichiometry.

It is well known [21] that the conventional procedure for the synthesis of such Ni LTM compounds includes the coprecipitation of water-soluble components, for example, nickel nitrate and ammonium paramolybdate, at different pH, solution concentrations, and Ni : Mo atomic ratios.

We were the first to synthesize analogous compounds by the mechanochemical activation of a solid-phase mixture of nickel hydroxocarbonate and ammonium paramolybdate. Duplyakin et al. [15] demonstrated that, in the process of mechanochemical activation in the range of selected process parameters, NHC was disintegrated to a size of  $0.1\text{--}0.2\ \mu\text{m}$  and a plastic flow regime was established for APM. Under the conditions of mechanical action, APM particles softened and covered NHC particles to interact with crystal water and to partially dissolve in it. In this case, as a result of the accumulation of extensive defects in the NHC particles in the course of mechanochemical activation and the dissolution of APM, the resulting charged ions  $\text{Ni}^{2+}$  and  $\text{MoO}_4^{2-}$  chemically interacted with the formation of layered Ni LTM compounds. Then, the mechanochemical synthesis of  $\beta\text{-NiMoO}_4$  could be easily performed in the mixture of the com-

pounds having a layered structure. Under the action of shear stress in an activator mill, layered compounds underwent fragmentation along the layers to cause the layer-by-layer mixing of the reagents as a result of plastic deformations with the formation of a solid solution of NiO in nickel molybdate upon the subsequent calcination at temperatures of  $470\text{--}520^\circ\text{C}$ . This fact led to the formation of the phase of  $\beta\text{-NiMoO}_4$ , which is stable at room temperature.

Using an approach described in [21, 22], we calculated the composition of Ni LTM compounds for different Ni : Mo atomic ratios. Table 3 summarizes the results of the calculation. The results of the quantitative evaluation of the phase composition and IR spectra of products after mechanochemical activation and calcination at  $520^\circ\text{C}$  are also given in Table 3.

As can be seen in Table 3, all of the tested mechanically activated compositions have the phase of  $\beta\text{-NiMoO}_4$  as a constituent regardless of the Ni : Mo atomic ratio. In this case, the amount of  $\beta\text{-NiMoO}_4$  in the mixture changed for different values of  $m$ . The mechanically activated and calcined mixture with the atomic ratio  $m = 1.4$  consisted of pure  $\beta\text{-NiMoO}_4$ . A decrease in the Ni : Mo atomic ratio to a stoichiometric value ( $m = 1$ ) led to the appearance of 18%  $\alpha\text{-NiMoO}_4$  and a corresponding decrease in the concentration of  $\beta\text{-NiMoO}_4$  in the composition to 82%. The presence of a large excess of NHC ( $m = 3.3$ ) made the composition X-ray amorphous, and free nickel oxide was a constituent of this composition. With an excess of APM ( $m = 0.3$ ), a large portion of the product (54%) consisted of free molybdenum oxide and two modifications of nickel molybdate.

Thus, based on this study, we can conclude that the use of mechanochemical activation in the synthesis of nickel molybdates makes it possible to synthesize the product containing 70–100% of thermally stable  $\beta\text{-NiMoO}_4$ .

## ACKNOWLEDGMENTS

We are grateful to N.V. Antonicheva and T.V. Kireeva (Institute of Hydrocarbon Processing, Siberian Branch, Russian Academy of Sciences) for performing thermal analysis and determining metals by AAS, respectively.

This work was supported by the Ministry of Science and Education (state contract no. 02.740.11.0647 of March 29, 2010).

## REFERENCES

1. Pillay, B., Mathebula, M.R., and Friedrich, H.B., *Appl. Catal.*, A, 2009, vol. 361, p. 57.
2. Sleight, W. and Chamberland, B.L., *Inorg. Chem.*, 1968, vol. 7, p. 1672.
3. Plyasova, L.M., Ivanchenkov, I.Yu., Andrushkevich, M.M., Buyanov, R.A., Interberg, I.Sh., Khramova, G.A., Karakchiev, L.G., Kustova, G.N., Stepanov, G.A., Tsailingol'd, A.L., and Pilipenko, F.S., *Kinet. Katal.*, 1973, vol. 14, no. 4, p. 1010.
4. Mazzocchia, C., Del Rosso, R., and Centola, P., *An. Quim.*, 1980, vol. 79, p. 108.
5. Pilipenko, F.S. and Stepanov, G.A., *Kinet. Katal.*, 1976, vol. 17, no. 4, p. 842.
6. Chaturvedi, S., Podriguez, J.A., Hanson, J.C., Albornoz, F., and Brito, J.L., Properties of Pure and Sulfided  $\text{NiMoO}_4$  and  $\text{CoMoO}_4$  Catalysts: TPR, XANES, and Time-Resolved XRD Studies. [http://www.mrs.org/s\\_mrs/inex.asp](http://www.mrs.org/s_mrs/inex.asp)
7. Levin, D., Soled, S.L., and Ying, J.Y., *Inorg. Chem.*, 1996, vol. 35, p. 4191.
8. Brito, J.L., Barbosa, A.L., Albornoz, A., Seveino, F., and Laine, J., *Catal. Lett.*, 1994, vol. 26, p. 329.
9. Brito, J.L. and Barbosa, A.L., *J. Catal.*, 1997, vol. 171, p. 329.
10. Laine, J. and Pratt, K.C., *React. Kinet. Catal. Lett.*, 1979, vol. 10, p. 207.
11. US Patent 6 534437 B2, 2003.
12. Molchanov, V.V. and Buyanov, R.A., *Usp. Khim.*, 2000, vol. 69, no. 5, p. 476.
13. Huirache-Acuna, R., Flores, Z.M.I., Albiter, M.A., Estrada-Guel, I., Ornelas, C., Paraguay-Delgado, F., Rico, J.L., Bejar-Gomez, L., Alonso-Nunez, G., and Martinez-Sanchez, R., *J. Mater. Online*, 2006, vol. 2. doi 10.2240/azoiomo0224
14. Avakumov, E.G., *Khim. Interes. Ust. Razv.*, 1994, no. 2, p. 541.
15. Duplyakin, V.K., Baklanova, O.N., Chirkova, O.A., Antonicheva, N.V., Arbusov, A.B., Voitenko, N.N., Drozdov, V.A., and Likhobolov, V.A., *Kinet. Catal.*, 2010, vol. 51, no. 1, p. 126.
16. Madeira, L.M., Portela, M.F., and Mazzocchia, C., *Catal. Rev.*, 2004, vol. 45, no. 1, p. 53.
17. Krylov, O.V. and Kiselev, V.F., *Adsorbsiya i kataliz na perekhodnykh metallakh i ikh oksidakh* (Adsorption and Catalysis on Transition Metals and Their Oxides), Moscow: Khimiya, 1988.
18. *Sovremennaya kolebatel'naya spektroskopiya neorganicheskikh soedinenii* (Contemporary Vibrational Spectroscopy of Inorganic Compounds), Yurchenko, E.N., Ed., Novosibirsk: Nauka, 1990.
19. Yurchenko, E.N., Kustova, T.N., and Batsanov, S.S., *Kolebatel'nye spektry neorganicheskikh soedinenii* (Vibrational Spectra of Inorganic Compounds), Novosibirsk: Nauka, 1981.
20. Andrushkevich, M.M., Buyanov, R.A., Khramova, G.A., Sitnikov, V.G., Itenberg, I.Sh., Plyasova, L.M., Kustov, G.N., Stepanov, G.A., Tsailingol'd, A.L., and Pilipenko, F.S., *Kinet. Katal.*, 1973, vol. 14, no. 4, p. 1015.
21. Levin, D. and Ying, J.Y., *J. Electroceram.*, 1999, vol. 3, no. 1, p. 25.
22. Levin, D., Soled, S.L., and Ying, J.Y., *Chem. Mater.*, 1996, vol. 8, p. 836.